ORIGIN OF RODINGITES IN ULTRAMAFIC ROCKS FROM LESVOS ISLAND (NE AEGEAN, GREECE)

K. Hatzipanagiotou*, B. Tsikouras*, G. Migiros, E. Gartzos**** and **K. Serelis****

***** *University of Patras, Department of Geology, Section of Earth Materials, GR-265 00 Patras, Hellas.*
****** *Agricultural University of Athens, Laboratory of Mineralogy-Geology, Iera Odos 75, GR-118 55 Athens, Hellas.*

Keywords: *rodingite, metasomatism, diffusional mass-transfer, ophiolite. Lesvos, Greece.*

ABSTRACT

Rodingite dykes occur in serpentinised harzburgites from the southern part of Lesvos Island (Aegean Sea). Based on relict primary textures and chemical data, doleritic protoliths are inferred. The rodingitic assemblage consists mainly of hydrogrossular, chlorite, diopside and epidote. In several cases, a chlorite reaction zone occurs at the rim to the host serpentinite.

The rodingitisation process developed in two stages: the formation of hydrogrossular + chlorite, and the formation of the diopside ± epidote and the chlorite reaction zone. This two-stage alteration is associated with the earlier formation of chrysotile + lizardite and then of antigorite, in the host serpentinite. There is a variable extent of element mobility in the rodingites, at constant mass, which is suggestive of diffusional mass-transfer. This behaviour is further supported by the mobility of Ti, Zr, Y and Cr, and the antithetic chemical exchange between the rodingite and the serpentinite. However, a major influence of a hydrothermal fluid phase is indicated by increase of silica activity at the second stage of metasomatism, when the diopside and the antigorite formed in the rodingite and the serpentinite, respectively. Moreover, alteration of the harzburgites cannot account as the only source of the significant Ca amounts required for the rodingitisation, and hence it is likely that considerable amounts of Ca^{+2} were introduced in the rodingite via a hydrothermal fluid. However, the relatively smaller volume of the rodingite compared to the harzburgite may also account for this Ca-enrichment. Hydrothermal circulation and diffusion were overlapping processes, but the first probably appeared during the second stage of rodingitisation.

Initial formation of hydrogrossular and chlorite requires influx of Ca into the system and depletion of Si, whereas subsequent formation of diopside requires influx of Mg. The chlorite reaction zone acted as a channel of high circulation of Mg- and H_2O-rich hydrothermal fluids.

No direct thermobarometric information can be obtained from the rodingite assemblage. However, considering that chrysotile + lizardite and antigorite are early and late products, respectively, during serpentinisation, their thermal stability fields (up to 350ºC for chrysotile + lizardite and 350-500ºC for antigorite) are suggestive for temperature increase, during the two stages of the rodingitisation.

INTRODUCTION

Rodingites have been reported from several ophiolite complexes (e.g. Capedri et al., 1978; Hatzipanagiotou, 1983; Tsikouras, 1994; Dubinska, 1995; 1997; Hatzipanagiotou and Tsikouras, 2001), as well as from Archean mafic sequences and present-day ocean floors (Honnorez and Kirst, 1975; Anhaeusser, 1979; Baltatzis, 1984; Schandl et al., 1989). They are interpreted as metasomatised Ca-rich and SiO_2-undersaturated rocks, usually associated with serpentinites (Coleman, 1977; Mittwede and Schandl, 1992). The petrogenetic process of rodingitization is rather debatable, as to whether the calcium necessary to produce their calc-silicate assemblages can be derived either from the Ca released during serpentinization (e.g. Coleman, 1977; O'Hanley et al., 1992), or by the circulation of hydrothermal fluids rich in Ca^{+2} ions, and/or leaching of the parent gabbroic rock (e.g. De, 1972; Hall and Ahmed, 1984). However, it is generally accepted that rodingitization of ophiolitic rocks is closely associated with the process of serpentinization.

This paper aims to describe in detail the mineralogical, textural and chemical features of some rodingite dykes found in serpentinites in Lesvos Island, to investigate their protoliths and to discuss their genetic evolution.

GEOLOGICAL SETTING

The lowermost sequence exposed in Lesvos Island comprises a pre-Alpine, low-grade metamorphic basement (Carboniferous to Middle Triassic; Hecht, 1972; Katsikatsos et al., 1986; Serelis, 1995; see Fig. 1). This basement includes schists with intercalations of metasandstones, quartzites and limestones.

An ophiolite mélange occurs above the crystalline basement via a tectonic contact. It is a chaotic and heterogeneous formation that consists of rock-fragments of variable composition, surrounded by a tectonised matrix. The frag-

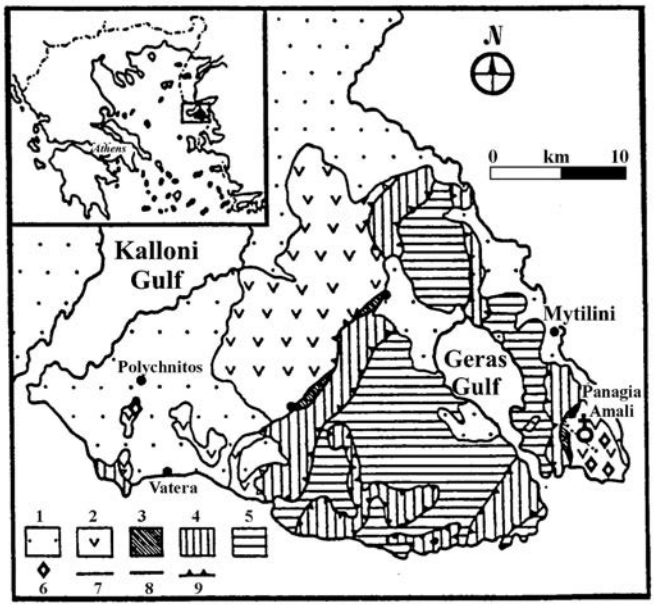

Fig. 1 - Geological sketch map of Lesvos Island (after Hecht 1972; Katsikatsos et al., 1986; and our own observations); 1- Quaternary and Neogene deposits, 2- Serpentinised peridotites, 3- Amphibolite sole, 4- Ophiolite mélange, 5- Metamorphic basement, 6- Rodingite localities, 7- Geological boundary, 8- tectonic contact, 9- thrust.

ments include ultramafic rocks, basalts, cherts, Triassic limestones and schists. The basalts within this mélange are bimodal: one group displays a within-plate affinity, similar to some Triassic volcanic rocks of Eastern Tethys, and a second group has mid-oceanic affinity, analogous to several ophiolitic basalts of the Aegean Sea (Tsikouras et al., 1994; Pe-Piper et al., 2001). Metasedimentary rock-fragments in this sequence display mineralogical parageneses of low greenschist facies (Katagas and Panagos, 1979).

Remnants of an ophiolite nappe are thrust over the ophiolite mélange. They contain mostly ultramafic rocks and minor dolerite dykes. The ultramafic rocks comprise intensively serpentinised lherzolites, harzburgites and minor dunites (Gartzos et al., 1992; Hatzipanagiotou and Pe-Piper, 1995; Migiros et al., 2000). The gabbroic dykes occur mostly in the southern parts of Lesvos (southern Amali Peninsula and Polychnitos area) and they intrude the serpentinised harzburgites. They dip steeply and display a thickness varying from some centimetres up to 1.5 m.

Locally, a medium to fine-grained amphibolite sole tectonically underlies the ophiolite. Hornblende separates from this sole have been radiometrically dated, suggesting a Late Jurassic age (153 ± 5 and 158 ± 5 Ma; Hatzipanagiotou and Pe-Piper, 1995).

On top of the pile there are Neogene lavas, pyroclastic rocks (Pe-Piper, 1980; 1984; Pe-Piper and Piper, 1992) and Quaternary deposits.

Rodingitised dykes

Rodingitic rocks are associated with gabbroic dykes occurring at southern Lesvos. Characteristic rodingite dykes were observed just a few metres westwards from the road that links the Vatera and Polychnitos villages, as well as at approximately 600 m southwards and 400 m eastwards from the Panagia Amali (see Figs. 1, 2a). The dykes occurring at Polychnitos are completely rodingitised while those found in the Amali peninsula often preserve relict gabbroic textures in the inner portions. The rodingite dykes are in sharp contact with the serpentinite host and frequently display a greenish, several centimetres thick, chloritic blackwall (Fig. 2b). In places, the rodingitised dykes are deformed and sometimes boudinaged.

PETROGRAPHY

Both the rodingites from the Amali peninsula and Polychnitos of southern Lesvos display common features. Due to incomplete re-equilibration, several domains of these rocks retain relics of their primary subophitic texture, which is suggestive of doleritic protoliths (Fig. 3a, b). Relics of primary clinopyroxene (mostly diopside), olivine and scarce plagioclase are frequent (Fig. 3b, c). The rodingite locally shows cataclastic textures as a result of brittle deformation, where mylonitised garnet is the most characteristic phase. Frequently garnet is pseudomorphic after plagioclase and displays corroded margins, suggesting that it is a rather early metasomatic phase (Fig. 3a, b, d). However, segregations of garnets are also dispersed in several places within the rodingite (Fig. 3c). The garnet is locally altered to a fine-grained aggregate of vuagnatite and rare paragonite (Fig. 3c, see also Mineral chemistry section). Vuagnatite ($CaAlSiO_4(OH)$) is a rare secondary mineral which developed within cracks of the garnets from the Lesvos rodingites or as pseudomorphs after garnet, forming admixtures with very fine grained paragonite. To our knowledge, the occurrence of vuagnatite has not been reported elsewhere in Greek rodingites.

Chlorite and tremolite replacing igneous clinopyroxene at rims and along cleavages may be interpreted as early alteration products. A second chlorite generation is also abundant in the rodingitic assemblage and is commonly associated with garnet.

Epidote (and clinozoisite) is also an early alteration product of igneous plagioclase, though in several samples, late epidote is commonly associated with neoblastic diopside.

The neoblastic diopside is the latest phase in the rodingitic assemblage and grows after garnet. Primary diopside relics are not easily distinguished from the neoblasts. Neoblastic diopside forms in general clearer and smaller crystals than the igneous relic clinopyroxenes. Due to this uncertainty, only a rough quantitative estimation for the neoblastic diopside of up to 10% of the mode can be made.

Accessory phases in the rodingite assemblage include titanite, magnetite and rare quartz grains. Veinlets filled with chlorite and epidote usually cut the rodingite.

The greenish blackwall mostly consists of chlorite, and very scarce titanite. The chlorite crystals are fine-grained and may display a weak preferred orientation towards the

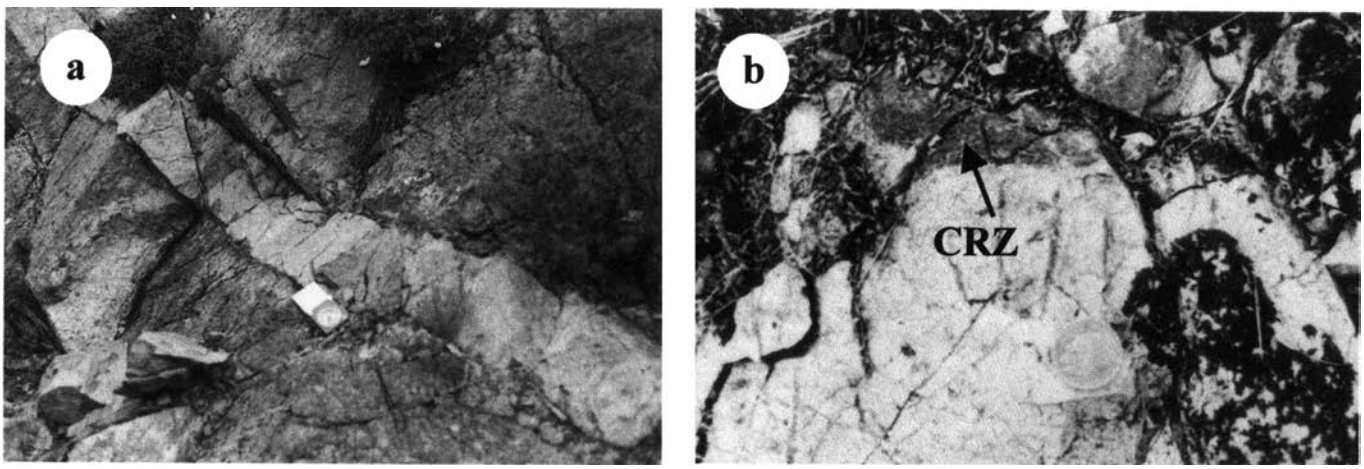

Fig. 2 - a) View of a rodingite dyke in serpentinised ultramafic rock; b) Detailed view of a rodingitic dyke with the chloritic reaction zone (CRZ).

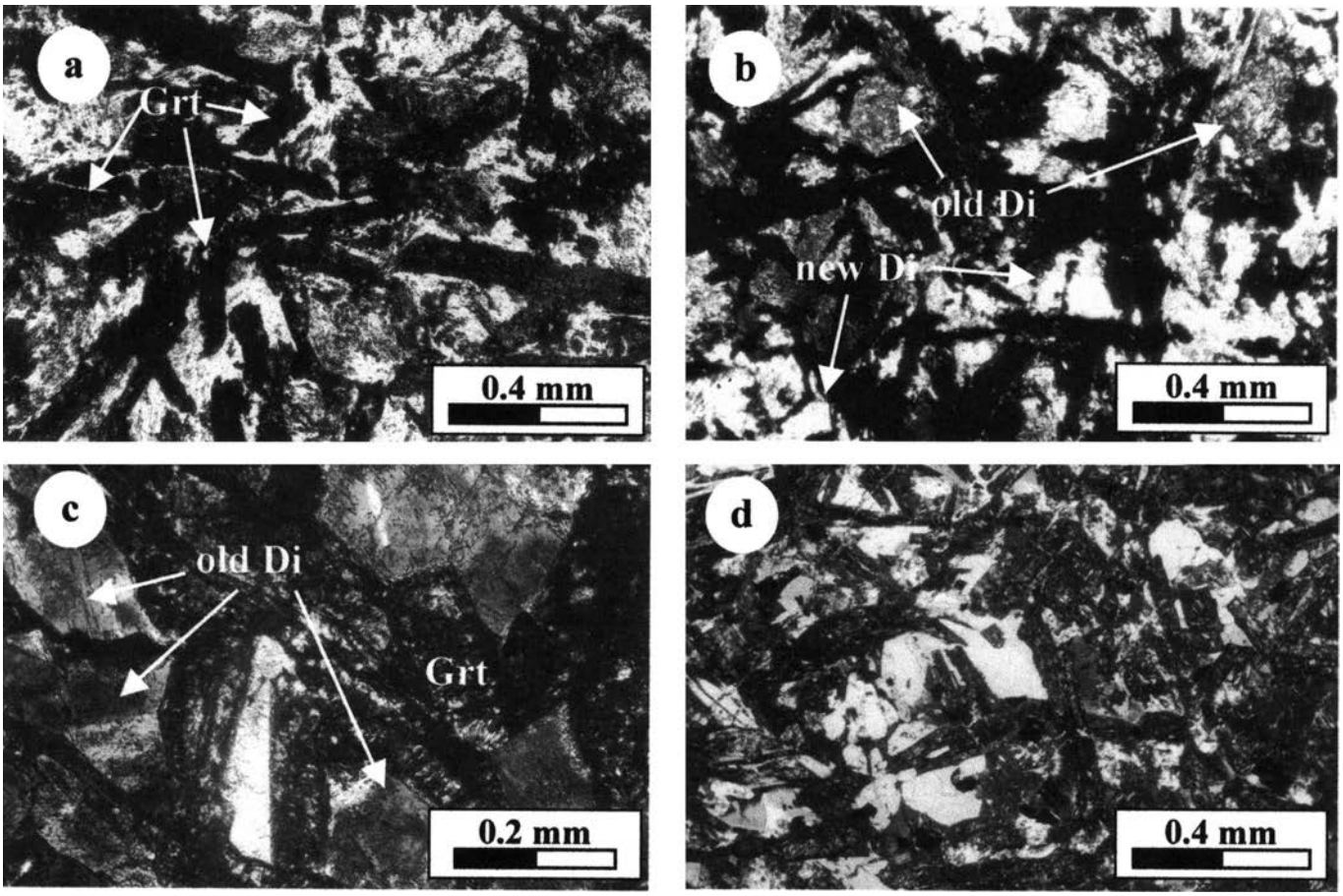

Fig. 3 - a) Relict subophitic texture in a rodingite from southern Lesvos. Garnet (Grt) replaced the plagioclase crystals. The bright crystals are relict igneous diopsides. Sample P 15b, Nicols +; b) Neoblastic diopside (new Di) forms clearer crystals than the relict igneous diopside (old Di) that displays a dusty appearance due to alteration, in the Lesvos rodingite. The lath-shaped crystals are hydrogrossulars, which pseudomorphically replaced plagioclase. Sample P 18, Nicols +. c) Garnet dispersed in the rodingite matrix. The very fine-grained crystals are a mixture of vuagnatite and paragonite. The larger crystals are igneous diopside. Sample 78, Nicols +. d) Neoblastic diopside (clear crystals) and pseudomorphic garnet after plagioclase (lath-shaped isotropic crystals) in a rodingite dyke still showing a relict subophitic texture. Sample 81, Nicols +.

rodingite, whilst towards the serpentinite, they become larger in size and are oriented almost perpendicular to the margins of the dykes.

Serpentinised harzburgites

Unaltered ultramafic rocks from the Lesvos ophiolite are rare, while most of the lower members of the suite are strongly serpentinised. These rocks have been deformed prior to serpentinization as it is indicated by the occurrence of relic kink-banded pyroxene porphyroclasts (and rarely olivine) and by formation of neoblastic pyroxene and olivine. The earliest phases are chrysotile and lizardite (pseudomorphic after olivine and pyroxene) that are locally replaced by irregular blades of antigorite, commonly associated with chlorite. Relics of primary spinel are common. Two generations of magnetite have been observed: the earlier one comprises primary hypidiomorphic to idiomorphic crystals and the latter includes secondary allotriomorphic grains formed after spinel and primary magnetite. Accessory phases include carbonates and talc commonly found in pods. Veins of carbonates, magnetite, clinozoisite and rare chalcedony are ubiquitous within the serpentinite and are likely related to late hydrothermal circulation.

ANALYTICAL METHODS

Mineral analyses were performed at the Department of Geology, University of Hamburg, Germany, with a CAMECA microanalyser, equipped with an Energy Dispersive System (EDS) and controlled by a Link system. Operating conditions were 15 kV accelerating voltage and 20 nA sample current.

Whole-rock chemical analyses were carried out at the Department of Earth Sciences, University of Leeds, England, using a PHILIPS PW 1400 XRF spectrometer. Fusion pellets were used for major-element and pressed powder pellets for trace-element determinations. Fe_2O_3 was determined by titration according to the method described by Wilson (1955).

MINERAL CHEMISTRY

Clinopyroxenes

Representative analyses of neoblastic clinopyroxenes are given in Table l. The analyzed crystals are diopside according to Morimoto et al. (1988). For comparison, a representative microprobe analysis of an igneous diopside is also listed (Table 1). The metasomatic diopside is richer in Ca and Ti, and poorer in Al and Na relative to the igneous one.

Table 1 - Representative microprobe analyses from the rodingites of Lesvos Island.

Clinopyroxenes				**Garnets**							**Chlorites**								**Epidotes**			**Vuagnatite**	
	Igneous	**neoblastic**									**partly rodingitized**			**rodingites**									
Sample	55.84	54.1	54.2		28.106c	28.96i	28.95r	55.80c	55.89i	55.83r		54.16	83.84	55.106	55.77	77.41	78.60	78.61		78.58	78.62		54.30
SiO_2	53.79	52.04	51.26	SiO_2	39.74	39.47	37 .96	37.67	38.48	37.58	SiO_2	31.10	30.07	29.35	28.74	33.46	26.17	25.83	SiO_2	38.38	38.38	SiO_2	32.71
TiO_2	--	0.11	0.13	TiO_2	--	--	--	--	--	--	Al_2O_3	17.34	20.99	20.14	19.75	13.37	20.73	21.13	TiO_2	0.05	0.09	Al_2O	28.97
Al_2O_3	3.18	1.43	1.75	Al_2O_3	22.42	22.18	21.89	23.58	22.14	21.77	Cr_2O_3	0.32	--	--	--	1.13	--	--	Al_2O_3	29.26	30.92	FeO	--
Cr_2O_3	0.10	0.31	0.35	FeO^t	0.56	0.49	2.72	0.61	0.19	1.02	NiO	0.04	0.12	0.09	0.11	0.10	0.04	0.07	Fe_2O_3	4.91	2.99	CaO	32.33
FeO^t	2.38	2.99	3.23	MnO	0.41	0.28	0.74	0.08	--	0.10	FeO	12.03	9.93	8.22	8.54	3.45	21.88	20.66	MgO	0.06	0.05	Na_2	0.02
MnO	0.09	0.13	0.12	MgO	--	--	0.78	--	--	1.56	MgO	27.85	27.12	29.14	28.71	33.31	17.68	17.17	MnO	0.05	0.16	Total	94.03
MgO	16.25	16.94	16.85	CaO	37.14	37.02	34.42	37.37	36.34	35.47	MnO	0.68	0.09	0.09	0.10	--	0.20	0.18	CaO	24.62	24.27		**4.5 O**
CaO	22.74	25.06	24.58	Total	100.27	99.44	98.51	99.31	97.15	97.50	CaO	0.12	0.11	0.05	0.04	--	0.17	0.04	Total	97.33	96.86	Si	0.973
Na_2O	1.93	0.17	0.16				**12 O**				Na_2O	0.04	0.12	--	--	--	--	--		**12.5 O**		Al	1.015
Total	100.46	99.18	98.43	Si	2.978	2.982	2.901	2.842	2.970	2.877	Total	89.52	88.55	87.08	85.99	84.82	86.87	85.08	Si	2.987	2.977	Fe	--
		6 O		Al^{IV}	0.022	0.018	0.099	0.158	0.030	0.123				**28 O**					Al^{IV}	0.013	0.023	Ca	1.030
Si	1.921	1.908	1.894		3.000	3.000	3.000	3.000	3.000	3.000	Si	5.981	5.751	5.674	5.645	6.482	5.467	5.473		3.000	3.000	Na	0.001
Al^{IV}	0.079	0.062	0.076	Al^{VI}	1.957	1.955	1.871	1.936	1.983	1.840	Al^{IV}	2.019	2.249	2.326	2.355	1.518	2.533	2.527	Al^{VI}	2.669	2.801		3.019
	2.000	1.970	1.970	Ti	--	--	--	--	--	--		8.000	8.000	8.000	8.000	8.000	8.000	8.000	Ti	0.003	0.005		
Al^{VI}	0.055	--	--	Fe^{3+}	0.035	0.031	0.174	0.038	0.012	0.065	Al^{VI}	1.908	2.479	2.259	2.213	1.532	2.567	2.745	Fe^{3+}	0.287	0.174		
Ti	--	0.003	0.004		1.992	1.986	2.045	1.974	1.995	1.905	Fe	1.935	1.588	1.329	1.403	0.559	3.823	3.661	Mg	0.007	0.006		
Cr	0.003	0.009	0.010	Fe^{2+}	--	--	0.045	--	--	--	Ni	0.006	0.018	0.010	0.017	0.016	0.007	0.012	Mn	0.003	0.011		
Fe^{3+}	--	--	--	Mg	--	--	0.089	--	--	0.178	Cr	0.049	--	--	--	0.173	--	--		2.969	2.997		
Fe^{2+}	0.071	0.092	0.100	Mn	0.026	0.018	0.048	0.005	--	0.006	Mg	7.984	7.733	8.938	8.406	9.621	5.506	5.423	Ca	2.053	2.017		
Mg	0.865	0.926	0.928	Ca	2.982	2.996	2.818	3.020	3.005	2.910	Mn	0.111	0.015	0.015	0.017	--	0.035	0.032					
Mn	0.003	0.004	0.004		3.008	3.014	2.955	3.025	3.005	3.094	Ca	0.025	0.023	0.010	0.008	--	0.038	0.009	Pistacite	9.67	5.80		
Ca	0.870	0.984	0.973	Alm.	--	--	--	--	--	--	Na	0.015	0.045	--	--	--	--	--					
Na	0.134	0.012	0.011	And.	1.76	1.56	8.50	1.95	0.62	3.43													
	2.001	2.030	2.030	Gros.	97.37	97.85	86.87	97.88	99.38	90.61		12.033	11.901	12.561	12.064	11.901	11.976	11.882					
Wo	48.10	49.07	48.54	Pyr.	--	--	3.01	--	--	5.75													
En	47.82	46.16	46.30	Spess.	0.87	0.59	1.62	0.17	--	0.21													
Fs	4.08	4.77	5.16																				

c- core, i- intermediate.

Garnet

Representative garnet microprobe analyses are listed in Table l. Fe^{+3}/Fe^{+2} partitioning was calculated on a stoichiometric basis; most iron in these garnets occurs in the trivalent state. The analyzed crystals are essentially pure grossular with only minor amounts of the andradite and spessartine components. Several microprobe totals tend to be less than 100% (see Table 1) indicating the existence of the hydrogrossular molecule. The garnets have a chemical zonation, which shows no systematic core-to-rim evolution. It can be inferred from Table 1 that most of the analysed elements display variable contents at the core, intermediate area and rim of the crystals. In general, there is an increase in Mg and a decrease in Fe^{+3} in the cores of the analysed crystals, reflected as increments in pyrope and decrease in andradite contents, respectively. This variation does not contradict a growth via oscillatory zoning, but unfortunately, no complete garnet profiles are available to establish such a hypothesis.

Epidote-clinozoisite, chlorite and vuagnatite

Epidote group minerals and chlorite occur both as matrix phases and in veins usually associated with the neoblastic clinopyroxene and garnet, respectively. Epidote is compositionally homogeneous having a rather low Fe^{+3} (stoichiometric calculations assuming total Fe as Fe^{+3}) and high Al contents and a narrow range of low pistacitic contents (5.80-9.67%). Chlorites from the rodingites have a rather broad $Fe^{tot}/(Fe^{tot}+Mg)$ variation, showing three distinct compositions (i.e. ripidolite, clinochlore, and penninite; see Table 1 and Fig. 4).

A representative microanalysis of vuagnatite is shown in Table 1 indicating a stoichiometry close to its ideal formula $CaAlSiO_4(OH)$. The vuagnatite probably accommodates Ca released during the alteration of garnet (identification of vuagnatite was also tested by XRD analysis). Microprobe analyses of paragonite are not reported here, because they are of low quality due to extremely small crystal size.

Whole-rock geochemistry

Bulk rock analyses of the rodingites of Lesvos Island are displayed in Table 2. An average of 6 fresh dolerites from the Lesvos ophiolite, which gives an approximation of the unrodingitised material, is given as a representative composition of the rodingitic protolith. Evidently, the rodingites are poorer in SiO_2, Na_2O and K_2O and richer in CaO contents relative to the inferred protolith.

On the ACF diagram, the studied rodingites plot away from the Coleman's (1977) rodingitic field, but they can be correlated with analogous rocks from the Abitibi Greenstone Belt, Canada (Schandl et al., 1989), which derived from metasomatism of mafic and ultramafic rocks (Fig. 5). Deviation of the rodingite compositions from the "rodingitic" field is common, thus its validity has been strongly argued and the variable chemistry of rodingites has been ascribed to variatons in chemistry, mineral assemblage and degree of metasomatism of their protoliths (e.g. Capedri et al., 1978; Wares and Martin, 1980; Rice, 1983; Schandl et al., 1989; O'Hanley et al., 1992; Dubinska, 1997). The unmetasomatised average dolerite composition plots in the three phase field of clinozoisite + clinochlore + actinolite, consistent with the incipient greenschist-facies, ocean-floor alteration of this assemblage that includes epidote + chlorite + tremolite. The bulk composition of the metasomatized rocks is shifted towards the AC tie line leading to the possible stable coexistence of epidote together with diopside and grossularitic garnet. The apparent distribution of the rodingite samples parallel to the C-F tie line of the ACF diagram (Fig. 5) would reflect both the strong influence of grossular on the chemistry and different extents of rodingitisation (O'Hanley, 1996). As it is expected, the composition of the chloritic reaction rim plots close to the clinochlore composition.

A well-developed chloritic reaction zone, from a dyke in the Vatera area, was chosen for the study of the metasomatic exchanges. Three chemical analyses of a traverse from a rodingite and the reaction zone to the host serpentinite (analyses P 17A2, P 17A1 and P 158, respectively) are shown in Table 2. The bulk-rock chemistry of the serpentinite, particularly the low Cr, Ni, Al and Ca contents, is com-

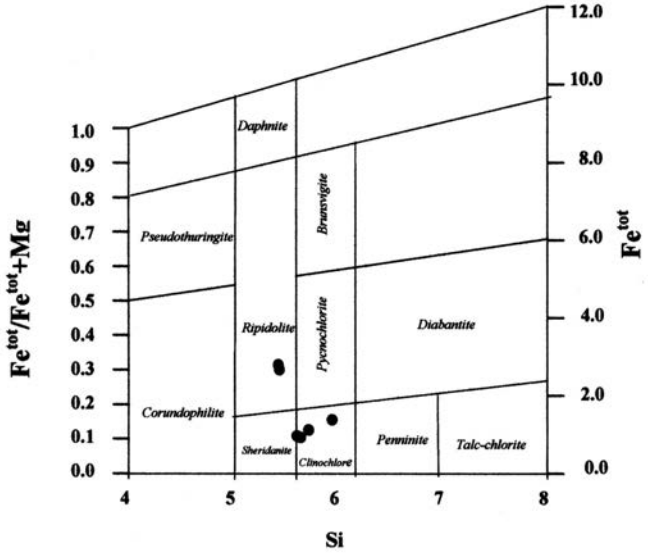

Fig. 4 - Plot of the analyzed chlorites from the south Lesvos rodingites, on the classification diagram (after Hey, 1954).

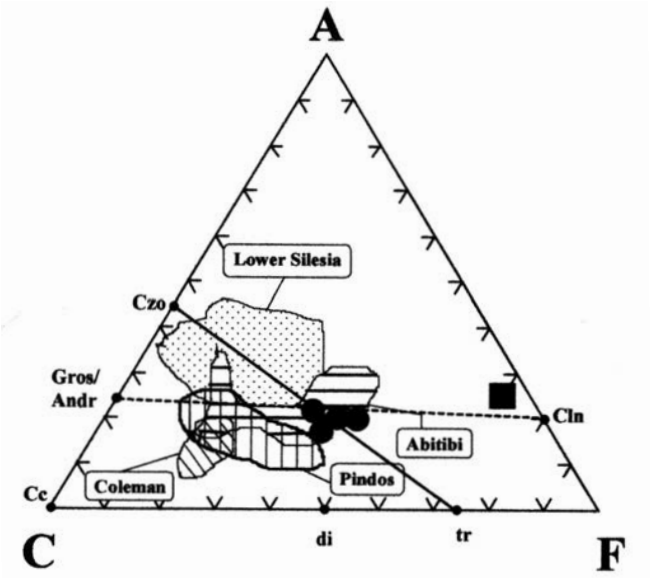

Fig. 5 - ACF diagram for the analyzed rodingites. For comparison, the fields from other rodingite localities as well the "rodingitic field" after Coleman (1977) are shown. (Data after Capedri et al., 1978: Pindos; Schandl et al., 1989: Abitibi; Dubinska, 1997: Lower Silesia). Circles: rodingites; square: chlorite reaction zone.

Table 2 - Representative whole-rock chemical compositions of the Lesvos rodingites and dolerite.

Major elements %

Sample	P 15C	P 17A	P 33	P 67	P 17A2 (internal)	P 17A1 (rim)	P 158 (serpen.)	Average dolerite
SiO_2	35.40	35.30	35.36	36.78	35.39	28.74	40.08	45.90
TiO_2	1.29	0.88	1.12	1.17	1.20	0.99	0.02	1.63
Al_2O_3	14.48	17.58	15.60	14.58	14.88	21.50	0.58	15.18
FeO	2.76	1.31	1.99	2.12	1.91	10.20		6.69
Fe_2O_3	7.25	4.10	5.84	5.33	6.18	4.62	*7.20	3.11
MnO	0.13	0.05	0.08	0.07	0.06	0.01	0.03	0.15
MgO	13.96	12.61	14.50	14.48	16.58	22.21	37.94	7.18
CaO	17.59	19.11	17.50	18.86	15.66	2.03	0.17	10.20
Na_2O	--	--	--	--	--	--	--	3.28
K_2O	0.17	--	0.08	--	--	--	--	0.33
P_2O_5	0.08	--	0.07	0.05	0.05	--	0.06	0.20
LOI	7.40	7.20	7.70	7.18	8.50	10.70	12.60	5.45
Total	100.51	98.14	99.84	100.62	100.68	101.00	98.68	99.31

Trace elements ppm

Ba	522	188	280	102	99	36	--	171
Rb	9	--	--	--	--	--	--	8
Sr	32	22	28	18	30	4	8	96
Y	35	28	36	26	44	30	--	28
Zr	67	35	51	55	50	31	--	111
Nb	--	--	--	--	--	--	--	9
Th	--	10	--	--	--	--	n.d.	n.d.
Ga	--	9	7	8	7	8	--	n.d.
Zn	43	15	27	38	23	24	43	n.d.
Cu	8	5	6	5	5	4	--	n.d.
Ni	221	380	348	322	442	867	2545	118
V	230	201	231	221	263	341	n.d.	n.d.
Cr	405	429	498	514	661	683	2210	280

Normative mineralogy
Sample: P 158

Q	--	Ab	--	Lc	--	Ol	59.45	il	0.04
C	0.48	An	0.53	Di	--	mt	1.74	ap	0.15
Or	--	Ne	--	Hy	37.19	hm	--		

-- below detection limit; * total Fe as Fe_2O_3; n.d. not determined; Average dolerite: mean values from 6 dolerite samples (data after Tsikouras et al., 1994).

parable with harzburgites from Alpine peridotites. The normative composition, calculated following the method of Lensch (1968), argues also for a harzburgitic protolith (Table 2). Ti and Cr contents are similar in both the reaction rim and the rodingite (Fig. 6). Very low Mn concentrations and total depletion of alkalies, along with Rb are common features of all rocks. Si is enriched in both the rodingite and the serpentinite but depleted in the chlorite reaction rim, whereas Ca is clearly high in the rodingite and low in both the chlorite reaction rim and the serpentinite host (Fig. 6).

DISCUSSION

Initial serpentinization of peridotites and simultaneous rodingitization of dykes typically occur in an oceanic environment, in ophiolitic rocks wordwide, as has been reported in many ophiolites ranging in age from Archean to Pleistocene (e.g. Laurent, 1980; Schandl et al., 1989; O'Hanley et al., 1992; Dubinska, 1997; Hatzipanagiotou and Tsikouras, 2001). The observed assemblages in the Lesvos rodingites are similar to those from worldwide Phanerozoic rodingites. Chlorite, epidote and tremolite are typical phases that first appear during an incipient, ocean-floor metamorphic episode. The rodingites are temporally associated with ocean-floor metamorphism. However, unlike the assemblages observed in ocean-floor metamorphic rocks worldwide, which are consistent with growth via interactions of low-pH solutions with the country-rock, the rodingitic assemblages are related to high pH solutions (Bird et al., 1984). The formation of grossular and a second chlorite generation which appeared during rodingitisation processes in Lesvos Island, was apparently induced by high activity of Ca^{+2} in a highly alkaline environment (Barnes et al., 1972;

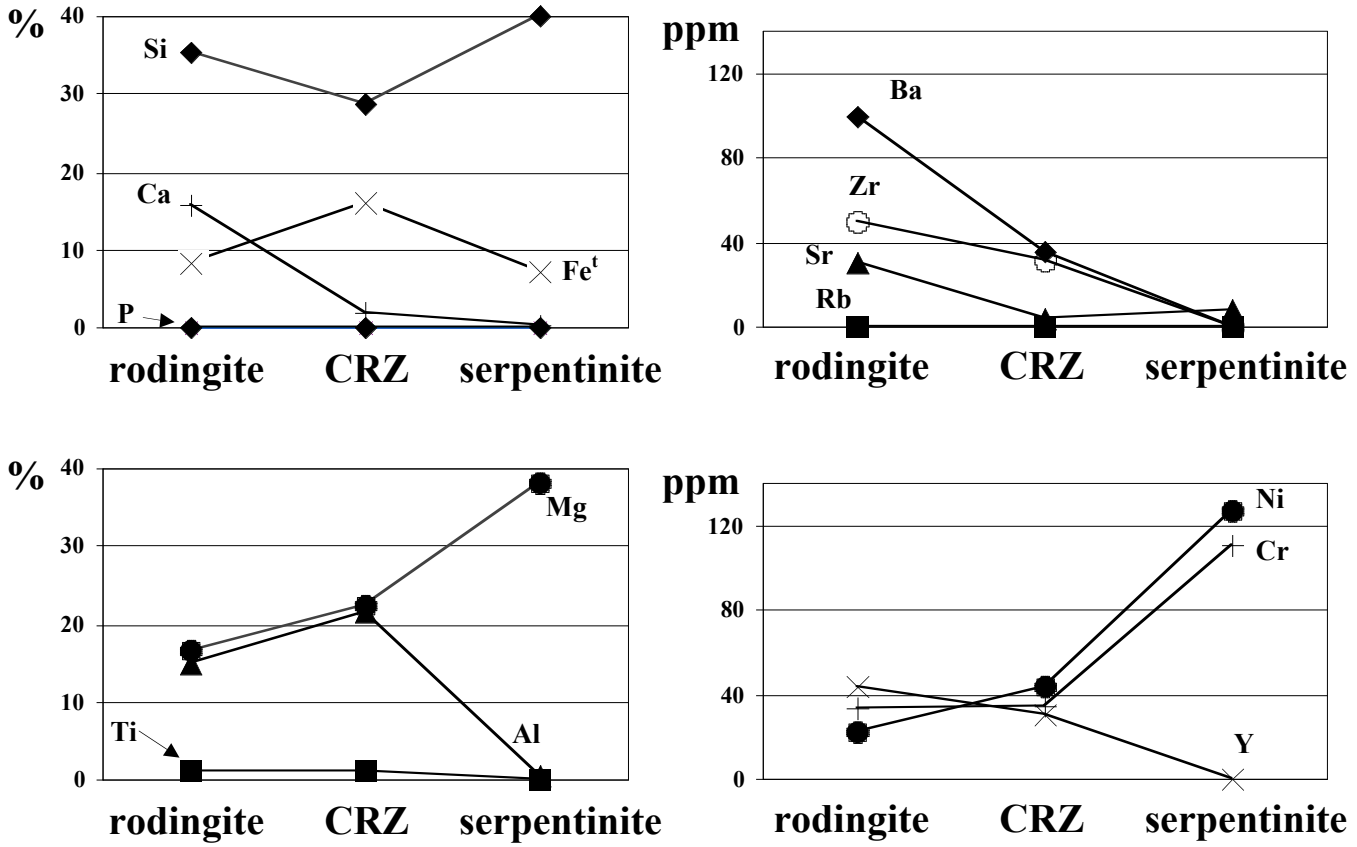

Fig. 6 - Chemical variations across a reaction zone between the rodingite protolith and the serpentinised ultramafic rock, from the Polychnitos area (CRZ-chlorite reaction zone); major elements as wt% of oxides;

1978). A second stage of metasomatism involves Mg- and Si-increase to produce diopside ± epidote.

The onset of rodingitization is marked by the appearance of grossular/hydrogrossular at the expense of plagioclase, and may be described by a reaction proposed by Coleman (1967):

$$CaAl_2Si_2O_8 + 2\ Ca^{+2} + 3\ H_2O + 0.5\ SiO_2 \leftrightarrows Ca_3Al_2Si_{2.5}O_{10}(OH)_2 + 4\ H^+$$

(anorthite) (hydrogrossular)

Furthermore, the crossed tie line relation indicated by the dashed line in Figure 4 represents the reaction:

$$16\ \text{clinozoisite} + 3\ \text{tremolite} + 25\ CaO + H_2O \leftrightarrows 3\ \text{clinochlore} + 21\ \text{grossular}$$

Both reactions imply hydration by a fluid that has been rich in Ca^{+2} ions and model the appearance of metasomatic garnet and chlorite. Studies from rodingites suggest that this metasomatic event may occur at pressures between 0.25 and 3 kbars (O'Hanley et al., 1992; Mittwede and Schandl, 1992; Schandl et al., 1989).

Schandl et al. (1989) describe a sequence of assemblages in rodingites, which develop at different extents of metasomatism and include, towards the most advanced alteration stages:

i) Epidote-rich rodingites (with the assemblage clinozoisite, zoisite and minor diopside and titanite)
ii) Grossular-rich rodingites (with the assemblage hydrogrossular, prehnite and minor diopside), and
iii) Diopside-rich rodingites.

The mineral assemblage of the Lesvos rodingite correlates with the second one or an intermediate between the second and the third alteration stages. Formation of diopside in the rodingites, suggests a relatively advanced stage of alteration, and it is probably associated with the formation of antigorite, after lizardite and chrysotile, in the host serpentinite.

Bulk chemical compositions of the rodingites were used to document the relationships between Ca-metasomatism and element mobility. Since the patterns of losses and gains during oceanic hydrothermal alteration are quite different from those produced by rodingitic alteration, the compositional trends correlating with gross variation in CaO are regarded as having been imposed by rodingitization. Independence from CaO suggests stable behaviour during this process. Linear variation trends of several elements versus CaO suggest that most of them behaved as mobiles with the exception of Al and Zr that show no particular correlation with CaO (Fig. 7).

The isocon method (Grant, 1988) was used as an attempt to present a qualitative estimation of losses and gains during rodingitization (Fig. 8). This is a graphical approach to the mass transfer equation used by Gresens (1967) to determine element mobility in metasomatised rocks. According to this technique, when the composition of unaltered and altered rocks plot as variables, the immobile elements during a metasomatic episode must lie on a straight line (isocon), which passes through the origin. The reciprocal slope gives the total mass change during the metasomatic process while the deviation of points for mobile elements above and below the isocon gives respectively the gain or loss of each component in the altered rock with respect to the concentration in the original.

We do not intend to calculate elemental losses and gains due to the uncertainty that arises from the lack of the actual protolith of the rodingites. Comparison of a rodingite (sample P 17 A2; altered) with the average dolerite (unaltered)

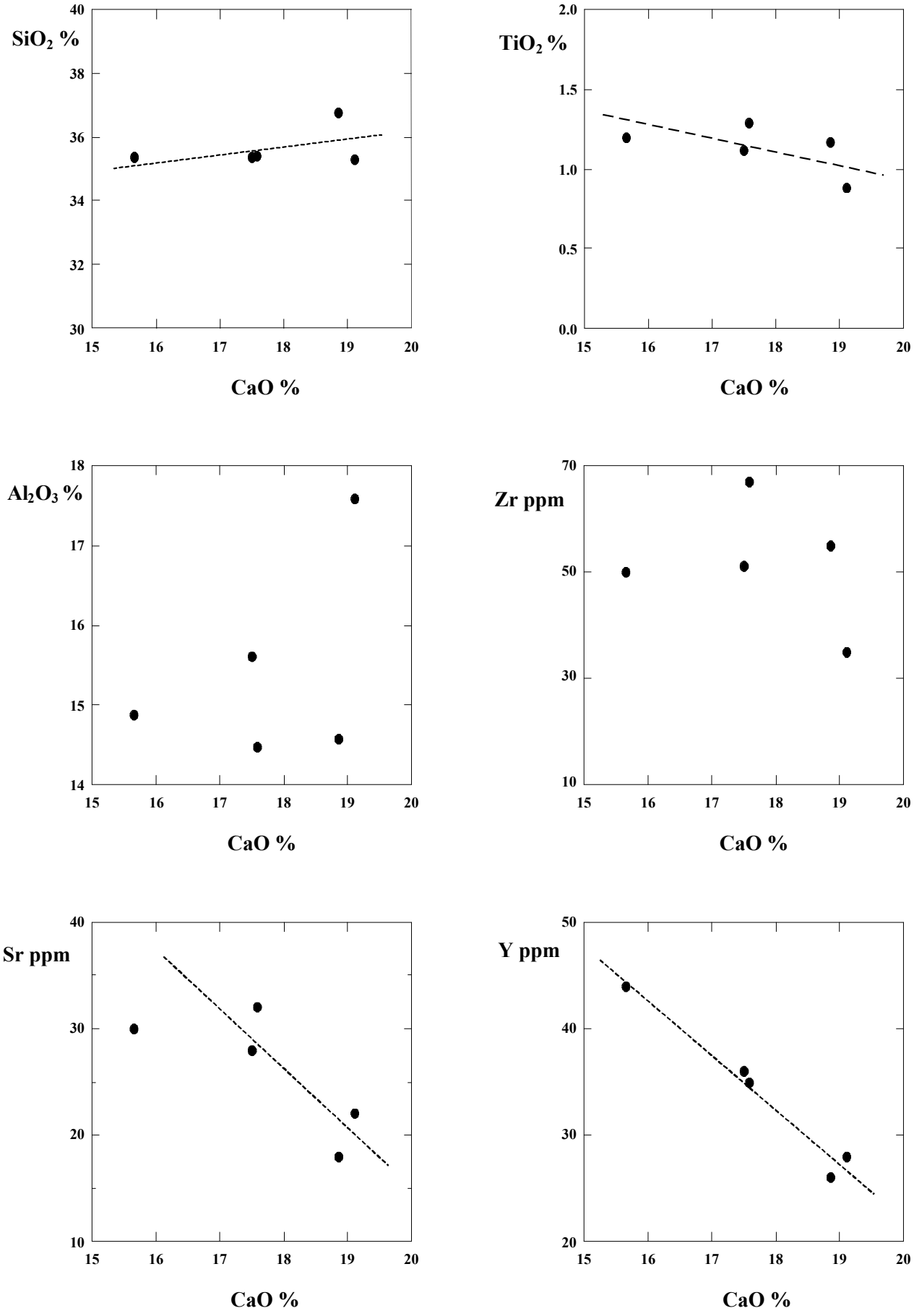

Fig. 7 - Correlation among selected elements and CaO contents in the Lesvos rodingites.

can only suggest a general qualitative determination of the pattern of element mobility during metasomatism, while calculation of gains and losses is meaningless. Evidently, mobility of all elements has occurred to a variable degree (i.e. the position of the elements above or below the isocon line shows variable extents of mobilization). The isocon line, assuming constant alumina alteration, has a slope of 0.98, implying a total mass gain of 2% (reciprocal ratio = 1.02) during the rodingitisation (Fig. 8). This very low value, which essentially intimates mass conservation during alteration, suggests that chemical exchanges during alteration occurred mainly by diffusional mass transfer between the rodingite and the serpentinite. Besides the predictable gain of Ca and losses of Si, K and Na, mobility of all other elements is obvious (Fig. 8). The considerable Fe_2O_3 gain is mostly counterbalanced by the FeO loss, thus only a small depletion of total iron is possibly required. This fact suggests that most Fe^{+2} was oxidised to Fe^{+3} rather than the Fe having been substantially mobilised. High f_{O2} conditions account for the oxidation of Fe. Such conditions are also suggested by the relatively high Fe^{+3} contents of most minerals in the rodingite, and also in the bulk chemistry of the rodingite itself.

An alternative hypothesis which assumes Zr or Ti immobility seems improbable since it will lead the isocon line to pass below the Si composition, thus requiring Si enrichment (see Fig. 8). However, such a scenario is unlikely, since Si-depletion processes typically affect rodingites. Mobility of Zr, Ti, Y and other icompatible elements has been established in the last decades, although in the past they were considered as immobile. These elements show a similar behaviour to REEs and can mobilize in hydrothermal systems when incorporated into low-pH solutions, in the presence of

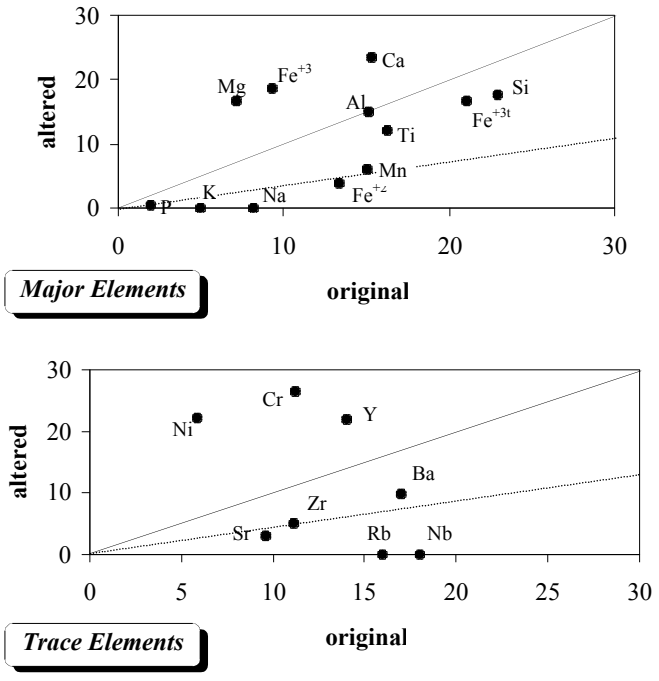

Fig. 8 - Isocon plots for major and trace elements using the method of Grant (1986) and assuming constant Al_2O_3 during alteration. "Original" refers to the average dolerite composition and "altered" refers to sample P 17A2. The data for major elements are plotted as weight percent of the oxides and trace elements in ppm. The dotted line represents an isocon assuming constant Zr. Scaling factors: SiO_2 (x 0.5), TiO_2 (x 10), FeO (x 2), Fe_2O_3 (x 3), $Fe_2O_3^t$ (x 2), MgO (x 1), MnO (x 10), CaO (x 1.5), Na_2O (x 2.5), K_2O (x 15), P_2O_5 (x 10), Ba (x 0.1), Rb (x 2), Nb (x 2), Sr (x 0.1), Zr (x 0.1), Y (x 0.5), Cr (x 0.04), Ni (x 0.05).

particular ions, such as chlorine, fluorine, phosphate and sulphate that act as ligands for forming polynuclear complexes (e.g. Gieré, 1986; 1990; Rubin et al., 1993). However, the rodingitic assemblage in Lesvos requires basic conditions of formation, therefore the mobility of Ti, Zr, Y, Cr, Ni is assigned to diffusional mass transfer rather than to infiltration of a fluid, as was also previously mentioned. The small length scale of the reaction zone is also consistent with the control of diffusion rather than infiltration on the mass transfer during rodingitisation (Brady, 1977).

However, simple diffusional mass-transfer cannot satisfactory explains the diffusion of components at a different extent. Thus, we have to assume that either this process has been controlled by the species which diffuse quickest (Brady, 1977) or that fluid infiltration was also operating. The first hypothesis is supported by the fact that there is an antithetic correlation between the changes in bulk-rock composition of the serpentinite and that of the rodingite. The early serpentinisation and formation of lizardite and chrysotile involves loss of Ca and gain of Si. However, the concomitant early formation of grossular and chlorite after plagioclase, epidote and tremolite show that Ca was added and Si was removed from the rodingite. The second stage involves the breakdown of chrysotile and lizardite to form antigorite (without producing brucite) and requires the serpentinite to have lost Mg and H_2O. In this case, the loss of Mg and H_2O from the serpentinite host is counterbalanced by the gain of Mg and H_2O from the rodingite, to produce the diopside and the chlorite reaction rim. Since the Cr/Ti values, used as an indicator as proposed by Sanford (1982), are rather similar in the rodingite and the chlorite reaction zone (0.09 and 0.11, respectively) we suggest that the latter formed at the expense of the dyke rather than of the host serpentinite (with Cr/Ti = 1.84). Petrographic observations, as well as major and trace element chemical variations across the reaction zone between the rodingite protolith and the serpentinised ultramafic rock are compatible with this interpretation. This reaction zone was probably a glass-rich rim of the dolerite dyke (chilled margin?), which allowed high circulation of the Mg- and H_2O-rich fluids.

The formation of diopside in the rodingite, as well as the formation of antigorite (and talc pods) within the serpentinite, imply an increase in $a(SiO_2)$ in both rock-types, which can be interpreted through the involvement of a hydrothermal fluid. In addition, the host harzburgite is normally poor in Ca and hence it represents a source of low potential in Ca for the significantly Ca-enriched rodingite. Therefore, the significant amounts of Ca^{+2} ions that entered the rodingite must have also been transported in a hydrothermal fluid phase. Hydrothermal circulation of Ca-rich fluids is also supported by the appearance of carbonate- and epidote-rich veins within the serpentinised harzburgites in several places of Lesvos Island (Serelis, 1995). Most likely, hydrothermal circulation overlapped difussion events, at least for a short period. As it was discussed earlier, the first process is mostly required for the second stage of rodingitisation (and the associated formation of antigorite in the serpentinite) and therefore it is considered as a late event. Another explanation for the Ca-enrichment in the rodingitised dykes is that it could be due to their relatively smaller volume compared to that of the host, "Ca-releasing" harzburgite. Based on the available data, both these factors may have contributed to the Ca-enrichment, however, further evidence, especially isotopic, is needed to clarify this point.

A broad estimation of the temperature of formation of

rodingite can be made on the basis of the formation of the serpentinite. Lizardite and chrysotile are stable at temperatures up to 350ºC (O'Hanley et al., 1987; Chernosky et al., 1988), whereas antigorite is stable between 350ºC and 500ºC; above 500ºC antigorite will recrystallize to forsterite + talc (O'Hanley et al., 1987). Furthermore, in the calculated phase diagram of O'Hanley et al. (1987) the reaction antigorite forsterite + talc + H_2O at 1 kbar is just below 500ºC and at 2.5 kbars it is slightly above 500ºC. Therefore, the sequential appearance of chrysotile-lizardite and antigorite in the associated serpentinite provides evidence for increasing temperature during rodingitisation. Furthermore, the absence of forsterite from the assemblage of the serpentinite is compatible with formation of the rodingites at temperatures lower than, or close to, 500ºC, depending on the pressure of formation.

CONCLUSIONS

Rodingite dykes occur in serpentinised ultramafic rocks at Polychnitos and the south Amali peninsula (southern Lesvos). Hydrogrossular and chlorite first appeared in the rodingite assemblage whereas diopside ± epidote subsequently grew after garnet. The late diopside development is temporarily associated with the formation of the chlorite reaction zone that rims several rodingite dykes. Relics of igneous textures in the rodingite suggest doleritic protoliths. The assemblage of the host serpentinite includes early-formed lizardite and chrysotile, which were subsequently overgrown by antigorite. The successive change in the studied rodingite mineralogy from CaAl-silicates to CaMg(±Al)-silicates is consistent with the two-stage serpentinization of the Lesvos ophiolite.

The chemistry of the rodingite dykes is also suggestive of metasomatic events after the inferred doleritic protolith. A qualitative study of element mobility, based on constant alumina alteration, shows typical Ca-enrichment and Si-removal, as well as considerable mobility of all other elements. The significant partition of Fe^{+3} in the rodingites and in the structural formula of the rodingite phases suggests alteration under relatively high f_{O2}. This is also evident from the apparent oxidation of Fe^{+2} to Fe^{+3}, indicated in the isocon plot. The isocon plot involves mass conservation, which is consistent with the control of diffusional mass-transfer during alteration. The mobility of certain elements, such as Ti, Zr, Y, Cr and Ni, is also assigned to diffusion, since the basic conditions of formation of the Lesvos rodingite are unfavourable for mobility of the above element via hydrothermal fluids. The antithetic geochemical correlations between the host serpentinite and the rodingite also support this hypothesis. Nevertheless, the increase in SiO_2 (during the second stage of alteration) and the depletion in alkalies in both the rodingites and the serpentinite, are more compatible with the contribution of an externally derived fluid. Moreover, alteration of the harzburgitic protolith of the associated serpentinite cannot account as the only source of the significant Ca amounts required for rodingitization. Therefore, it is likely that significant amounts of Ca^{+2} were introduced in the rodingite via a hydrothermal fluid. However, the Ca-enrichment in the Lesvos rodingites could also be due to their smaller volume relatively to the harzburgite that acted as the Ca source.

Estimation of temperatures of formation during the two stages of the rodingitisation can be grossly assessed from the serpentinite host. The lizardite-chrysotile-bearing assemblage (stable up to 350ºC) and the antigorite-bearing assemblage (stable in the range of 350-500ºC) provide evidence for increasing temperatures from the associated formation of grossular + chlorite to the concomitant stage of appearance of diopside, in the rodingite while absence of forsterite (stable above 500ºC) from the serpentinite assemblage provides an upper thermal limit for rodingite formation in Lesvos Island.

Acknowledgments

Review of an earlier manuscript by Professor Dr. M. Okrusch, as well as useful criticism and suggestions by an anonymous reviewer are gratefully acknowledged.

REFERENCES

Anhaeusser C.R., 1979. Rodingite occurrences in some Archean ultramafic complexes in the Barberton Mountain Land, South Africa. Precambrian Res., 36: 649-676.

Baltatzis E., 1984. A new occurrence of rodingite from Skiros Island, Greece. N. Jb. Miner. Mh., H7: 317-322.

Barnes I., O'Neil J.R and Trescazes J.J., 1978. Present day serpentinization in New Caledonia, Oman and Yugoslavia. Geochim. Cosmochim. Acta, 42: 144-145.

Barnes I., Rapp J.B. and O'Neil J.R., 1972. Metamorphic assemblages and the direction of flow of metamorphic fluids in four instances of serpentinization. Contrib. Mineral. Petrol., 35: 263-276.

Bird D.K., Schiffman P., Elders W.A., Williams A.E. and McDowell S.D., 1984. Calc-silicate mineralization in active geothermal systems. Econ. Geol., 79: 671-695.

Brady J.B., 1977. Metasomatic zones in metamorphic rocks. Geochim. Cosmochim. Acta, 41: 113-125.

Capedri S., Garuti G. and Rossi S., 1978. Rodingites from Pindos. Constraints on the "rodingite problem". N. Jb. Miner. Abh., 132: 242-263.

Chernosky J.V., Berman R.G. and Bryndzia L.T., 1988. Serpentine and chlorite equilibria. In: S.W. Bailey (Ed.), Hydrous phyllosilicates exclusive of micas, Reviews in Mineralogy, 19: 295-346.

Coleman R.G., 1967. Low-temperature reaction zones and alpine ultramafic rocks of California, Oregon and Washington. U.S. Geol. Surv. Bul., n. 1247.

Coleman R.G., 1977. Ophiolites, Ancient oceanic lithosphere? Springer-Verlag, Heidelberg New York, 229 pp.

De A., 1972. Petrology of dykes emplaced in the ultramafic rocks of southeastern Quebec and origin of rodingite. Geol. Soc. Am. Mem, 132: 489-501.

Dubinska E., 1995. Rodingites of the eastern part of Jordanow-Gogolow serpentinite massif (Lower Silesia, Poland). Can. Miner., 33: 585-698.

Dubinska E., 1997. Rodingites and amphibolites from serpentinites surrounding Sowie Gory block (Lower Silesia, Poland): Record of supra-subduction zone magmatism and serpentinization. N. Jb. Miner. Abh., 171: 239-279.

Gartzos E., Serelis K and Migiros G., 1992. Study of the amphibolitic rock unit of Lesvos Island (Greece). Ann. Geol. Pays Héllen., 35: 489-504.

Gieré R., 1986. Zirconolite, allanite and hoegbomite in a marble skarn from the Bergell contact aureole: implications for mobility of Ti, Zr and REE. Contrib. Mineral. Petrol., 93: 459-470.

Gieré R., 1990. Hydrothermal mobility of Ti, Zr and REE: Examples from the Bergel and Adamello contact aureoles (Italy). Terra Nova, 2: 60-67.

Grant J.A., 1986. The Isocon diagram - A simple solution to Gresens' equation for metasomatic alteration. Econ. Geol., 81: 1976-1982.

Gresens R.L., 1967. Composition-volume relationships of metasomatism. Chem. Geol., 2: 47-55.

Hall. A. and Ahmed Z., 1984. Rare earth content and origin of rodingites. Chem. Erde, 43: 45-56.

Hatzipanagiotou K., 1983. Die oberste Einheit des süd-ägäischen Deckenstapels auf Rhodos und Karpathos (Dodekanes/Griechenland): Relikte eines Ophiolith-Komplexes. Diss., TU Braunschweig, 163 pp.

Hatzipanagiotou K. and Pe-Piper G., 1995. Ophiolitic and sub-ophiolitic metamorphic rocks of the Vatera area, southern Lesbos (Greece): Geochemistry and geochronology. Ofioliti, 20: 17-29.

Hatzipanagiotou K. and Tsikouras B., 2001. Rodingite formation from diorite in the Samothraki ophiolite, NE Aegean, Greece. Geol. J., 36: 93-110.

Hecht J., 1972. Zur Geologie von Südost-Lesbos. Z. dt. Geol. Ges., 123: 423-492.

Hey M.H., 1954. A new review on the chlorites. Min. Mag., 224: 277-298.

Honnorez J. and Kirst P., 1975. Petrology of rodingites from equatorial Mid-Atlantic fracture zones and their geotectonic significance. Contrib. Mineral. Petrol., 49: 233-257.

Katagas C. and Panagos A., 1979. Pumpellyite-Actinolite and Greenschist facies metamorphism in Lesvos Island (Greece). TMPM, 261: 235-254.

Katsikatsos G., Migiros G., Triantaphyllis E. and Mettos A., 1986. Geological structure of internal Hellenides (E. Thessaly-SW Macedonia-Euboea-Attica-Northern Cyclades Islands and Lesvos). I.G.M.E. Geol. Geophys. Res., Sp. Issue, p. 191-212.

Laurent R., 1980. Regimes of serpentinization and rodingitization in Quebec Appalachian ophiolites. Arch. Sci. Genève, 33: 311-320.

Lensch G., 1968. Der normative Mineralbestand von Mafititen. N. Jb. Miner. Mh., 9: 306-320.

Migiros G., Hatzipanagiotou K., Gartzos E., Serelis K. and Tsikouras B., 2000. Petrogenetic evolution of ultramafic rocks from Lesvos Island (N. Aegean, Greece). Chem. Erde, 60: 27-46.

Mittwede S.K. and Schandl E.S., 1992. Rodingites from the southern Appalachian Piedmont, South Carolina, USA. Eur. J. Mineral., 4: 7 16.

Morimoto N., Fabriès J., Ferguson A.K., Ginzburg I.V., Ross M., Seifert F.A., Zussman, J., Aoki, K., Gottardi G. (1988). Nomenclature of pyroxenes. Am. Mineral., 73:1123-1133.

O'Hanley D.S., 1996. Serpentinites. Records of tectonic and petrological history. Oxford Monographs Geol. Geophys., 34, 277 pp.

O'Hanley D.S., Chernosky J.V. and Wicks F.J., 1987. The stability of lizardite and chrysotile. Can. Mineral., 27: 483-493.

O'Hanley D.S., Schandl E.S. and Wicks F.J., 1992. The origin of rodingites from Cassiar, British Columbia, and their use to estimate T and P (H_2O) during serpentinization. Geochim. Cosmochim. Acta, 56: 97-108.

Olesch M. 1978. Vesuvianite (idocrase) stability in the system CaO-MgO-Al_2O_3-SiO_2-H_2O up to 5 kbar. Abstracts IMA 10th Gen. Meet. Novos., 2: 177.

Pe-Piper G., 1980. Geochemistry of Miocene shoshonites, Lesbos, Greece. Contrib. Mineral. Petrol., 72: 387-396.

Pe-Piper G., 1984. Zoned pyroxenes from shoshonite lavas of Lesbos, Greece: inferences concerning shoshonite petrogenesis. J. Petrol., 25: 453-473.

Pe-Piper G. and Piper D.J.W., 1992. Geochemical variation with time in the Cenozoic high-K volcanic rocks of the island of Lesbos, Greece: significance for shoshonite petrogenesis. J. Volcan. Geotherm. Res., 53: 371-387.

Pe-Piper G., Piper D.J.W., Matarangas D. and Varti-Matarangas M., 2001. The sub-ophiolitic melange of the island of Lesbos, Greece. N. Jb. Miner. Mh., 6: 241-260.

Rice J.M., 1983. Metamorphism of rodingites: Part I. Phase relations in a portion of the system CaO-MgO-Al_2O_3-SiO_2-CO_2-H_2O. Am. J. Sci., 283-A: 121-150.

Rubin J.N., Henry C.D. and Price J.G. 1993. The mobility of zirconium and other "immobile" elements during hydrothermal alteration. Chem. Geol., 110 :29-47.

Sanford R., 1982. Growth of ultramafic reaction zones in greenschist to amphibolite facies metamorphism. Am J. Sci., 282: 543-616.

Schandl E.S., O'Hanley D.S. and Wicks F.J., 1989. Rodingites in serpentinized ultramafic rocks of the Abitibi Greenstone Belt, Ontario. Can. Mineral., 27: 579-591.

Serelis K., 1995. Investigation of the southern Lesvos ophiolite. Ph. D. Thesis, Agric. Univ. Athens, 238 pp.

Tsikouras B., 1994. Mineralogical and geochemical study of rodingites from Samothraki Island (N. Aegean). Bull. Geol. Soc. Greece, 30 (3): 63-77.

Tsikouras B., Beltas P. and Hatzipanagiotou K., 1994. Petrography and geochemistry of basaltic rocks from the Vatera ophiolitic melange (S. Lesvos, N. Aegean). Bull. Geol. Soc. Greece, 30 (3): 103-112.

Wares R.P. and Martin R.F., 1980. Rodingitization of granite and serpentinite in the Jeffrey mine, Asbestos, Quebec. Can. Mineral., 18: 231-240.

Wilson A.D., 1955. A new method for the determination of ferrous iron in rocks and minerals. Bull. Geol. Surv. GB, 9: 56-58.

Received, June 26, 2000
Accepted, May 23, 2003